ELSEVIER

International Journal of Mass Spectrometry and Ion Processes 164 (1997) 207–223

International Journal of Mass Spectrometry and Ion Processes

An investigation of electron attachment to $CHCl_2F$, $CHClF_2$ and CHF_3 using an electron-swarm mass spectrometric technique

G.K. Jarvis[a], C.A. Mayhew[a,*], L. Singleton[a], S.M. Spyrou[b]

[a]*Chemical Physics Laboratory, School of Physics and Space Research, University of Birmingham, Edgbaston, Birmingham B15 2TT, UK*
[b]*National Hellenic Research Foundation, Theoretical and Physical Chemistry Institute, 11635 Athens, Greece*

Received 14 March 1997; revised 1 May 1997; accepted 5 May 1997

Abstract

Non-thermal energy electron swarm attachment studies of the hydrochlorofluorocarbons $CHCl_2F$ and $CHClF_2$ and the hydrofluorocarbon CHF_3 have been carried out using an ion-mobility mass spectrometer. Mean electron energies from about 0.05 eV up to about 1.8 eV were covered by using a suitable choice of buffer gases and electric field strengths in the drift chamber of the instrument. Of the three molecules, only $CHCl_2F$ and $CHClF_2$ had measurable density normalised electron attachment coefficients over the range of mean electron energies covered. From these coefficients, electron attachment rate constants were determined as a function of mean electron energy. An unfolding technique has been applied to our measurements of the electron attachment rate constants of $CHCl_2F$ and $CHClF_2$ to obtain the total electron attachment cross section as a function of electron energy. Uniquely, the mass spectra of the anion products resulting from the electron attachment process and subsequent anion–molecule reactions in a swarm environment were measured with our apparatus, and these are reported.

Keywords: Electron attachment; cross sections; rate constants; electron swarms; SIFT

1. Introduction

Studies of electron attachment processes, identification of the product anions, and their yields for halogenated compounds have received considerable attention in recent years [1–6]. A major reason for this interest results from the presence of such compounds as contaminants in the atmosphere.

With the phasing out of chlorofluorocarbons (CFCs), hydrochlorofluorocarbons (HCFCs) and to some extent hydrofluorocarbons (HFCs) are being used in greater quantities as temporary replacements [7]. HCFCs and HFCs are predominantly removed in the troposphere by oxidation with hydroxyl (OH) radicals and to some extent removed in the lower stratosphere by free radical (OH and singlet atomic oxygen, $O(^1D)$) reactions and UV photolysis [8]. This limits their atmospheric lifetimes to a few years (compared to ~100 years for CFCs). Transport of these molecules into the upper atmosphere will therefore be minimised. Nevertheless, small quantities of HCFCs and HFCs will reach altitudes where reactions with charged species can take place. This draws attention to electron attachment mechanisms of the HCFCs and

* Corresponding author. E-mail: C.Mayhew@bham.ac.uk. Tel: 00 44 0121 414 3344. Fax: 00 44 0121 414 3722.

0168-1176/97/$17.00
PII S0168-1176(97)00060-8

HFCs in the upper atmosphere. Perhaps of more significance is the possible use of electrons as sensitive probes to the detection of these compounds in the troposphere. Current chemical ionisation techniques to measure the concentrations of HCFCs and HFCs might be improved if a detailed understanding of electron attachment processes is made available. Additional interest in the electron attaching processes of HCFCs and HFCs comes from their application to plasma processing (e.g. for microcircuit etching) and gaseous dielectrics. Electron attachment studies of HCFCs and HFCs are therefore very topical.

In this paper, we present an investigation of non-thermal electron attachment to two HCFCs, $CHCl_2F$ (HCFC-21) and $CHClF_2$ (HCFC-22), and one HFC, CHF_3 (HFC-23), over the mean electron energy range from about 0.05 eV up to about 1.8 eV. Our primary motivation for this study comes from the work of Christophorou and colleagues, which is summarised in a review by Christophorou et al. [1]. In their review, they present electron attachment rate constants as a function of the mean electron energy (0–1 eV) for a series of chlorine containing methanes, namely $CClF_3$, CH_2Cl_2, CCl_2F_2, $CHCl_3$, CCl_3F, and CCl_4, in a buffer gas of nitrogen. It is pointed out that, as a rule, the electron attachment rate constant increases with increasing Cl substitution. Furthermore, for a given number of Cl atoms in the molecule, replacement of H by F also increases the electron attachment rate constant. An aim of our study is to determine if electron attachment to the molecules $CHCl_2F$, $CHClF_2$ and CHF_3, obeys this rule, and if so over which mean energy range. We deliberately mention energy range, because there is an example of a break down of the rule in the data presented by Christophorou et al. For mean electron energies above 0.6 eV, the electron attachment rate constants for $CHCl_3$ are slightly greater than those for CCl_3F.

Another major stimulus for our study was to determine the electron attachment anion products, which until the development of our apparatus could not be determined under swarm conditions.

To our knowledge, there has been only one previous swarm study of the $CHCl_2F$ and $CHClF_2$ molecules [9], and this covers a mean electron energy from about 0.1 eV up to 0.8 eV. There have, however, been a number of studies dealing with the investigations of thermal energy electron attachment to $CHCl_2F$ and $CHClF_2$. For $CHCl_2F$ there are two reported measurements of the thermal-energy electron attachment rate [10,11], with the most recent one being that of Szamrej et al. [10]. They used a typical 'non-thermal' swarm technique but used a CO_2 buffer gas. This apparently provides a thermal electron energy distribution over the range $E/N = 0.6–9 \times 10^{-17}$ V cm^2 used in their experiments. (E/N is the ratio of the electric field strength, E, to the buffer gas number density, N, and is normally referred to as the reduced electric field.) The value they obtained for the thermal electron attachment rate constant is 7.4×10^{-13} cm^3 s^{-1}. This is in fair agreement with the value of 1.5×10^{-12} cm^3 s^{-1} measured by Christodoulides et al. using an electron cyclotron resonance technique [11]. Christodoulides et al. also measured the thermal electron attachment rate constant for the $CHClF_2$ molecule, and obtained a value of $<3.5 \times 10^{-13}$ cm^3 s^{-1}. This is in good agreement with a comparable value of $< 1.6 \times 10^{-13}$ cm^3 s^{-1} reported in an earlier study by Davis et al. [12] who used a swarm apparatus with zero electric field applied.

2. Experimental details and procedures

Several experimental methods have been used for electron attachment measurements including the flowing afterglow/Langmuir probe (FALP) [13–17], electron beam [18–20], and electron swarm [21–27]. A detailed discussion of these and other experimental methods used to study low energy electron attachment to molecules appears in a recent review by Chutjian et al. [28]. The FALP has been successfully used to

obtain absolute thermal-energy electron attachment rate constants and to identify the anion products. Electron beam and mass spectrometric techniques, have been extensively used to measure the intensities of anion products of electron–molecule collisions as a function of electron energy, with energies from about 0.1 eV up to tens of electron volts, yielding information on the relative electron attachment cross section as a function of electron energy. The electron swarm techniques have been used exclusively to measure absolute electron attachment rate constants as a function of *E/N* in various buffer gases.

Until recently, information on the reaction products from electron attachment processes taking place under electron swarm conditions (i.e. broad electron energy distributions and high buffer gas pressures) has been missing. However, such information is required if a detailed knowledge of electron attachment processes is to be obtained. Whilst beam measurements do provide details on anion products at specific electron energies, a direct comparison between swarm and electron beam techniques is not straightforward. For example, in the swarm technique, moderately short lived anions (which in the single collision conditions of a beam experiment would be unobservable) can be stabilised by multiple collisions with a buffer gas.

In a recent advance in electron swarm techniques, an instrument has been developed at the University of Birmingham that cannot only measure electron attachment rate constants, as is standard for a swarm apparatus, but which can also record the masses (or more correctly the *m/z* values) of the anion products. The experimental apparatus, its modes of operation and the operational procedures used to record data have been described in full detail in an earlier publication [29]. In brief, one part of the apparatus is an ion mobility spectrometer (IMS). The second part of the apparatus is a quadrupole mass analyser, coupled to the IMS by way of a differential pumping region. The mass analyser is used to mass identify the anion products of the electron attachment process.

Standard IMS instruments, mainly used for analytical work, are described in detail in the literature [30–32], and hence no description of these will be given here. Our IMS consists of a reaction drift chamber separated from an electron source by a Bradbury–Nielsen (B–N) grid. The IMS operates at an atmospheric pressure of buffer gas that continuously flows through the system and is vented to air. This flow system has a distinct advantage over the normal static conditions of a typical swarm apparatus. In a static chamber, a small quantity (usually 10^{-5} to 10^{-8} of the buffer gas density) of the target gas is added in known concentration into the reaction chamber. The ratio of a voltage output pulse with and without the attaching gas added is then used to obtain a measurement of the density normalised electron attachment coefficient (see below). This has two consequences. Firstly, partial pressure (electron attaching gas pressure) effects will not be immediately obvious. Secondly, more accurate results are obtained if a number of measurements are taken at various partial pressures of the attaching gas. Although swarm measurements at various partial pressures are taken, it is not straight forward to change the concentration of the attaching gas in the chamber, and the whole process is time consuming. In a flow system, the electron attaching gas can be introduced in the buffer gas flow at varying rates that can quickly and easily be adjusted. Therefore, the concentration of the attaching gas in the reaction drift chamber can be simply altered without the need to make up individual samples of varying concentrations for each measurement. Another advantage of the flow system is that a mass spectrometer system can be coupled to the electron attachment chamber, whilst keeping the pressure in the chamber constant. The major disadvantage of a flow system, for which large quantities of buffer gas are used, is that it is more difficult to purify the buffer gas, and high purity is needed if reliable electron

attachment rate constants are to be obtained. We will return to this point later.

Since the publication of our first paper describing the instrument [29], simple modifications to its electronics have increased the voltage range, −200 to −3500 V, over which the drift tube operates in nitrogen. This means that the E/N value can be varied from about 6×10^{-19} V cm^2 up to about 1×10^{-17} V cm^2. This range corresponds to a change in the mean electron energy from about 0.05 eV up to about 0.4 eV. Furthermore, improved electrical isolation of the electron source now permits us to operate in an argon buffer gas over a voltage range of −100 to −1500 V. (Previous attempts to operate in argon were unsuccessful due to electrical breakdown.) This voltage range in an argon buffer gas allows mean electron energies from about 0.5 eV up to about 1.8 eV to be covered with our current drift tube length of 13.6 cm.

Electrons are produced in our IMS via ionisation of the ambient buffer gas by an 11 mCi ^{63}Ni β-ray source. The electrons drift down towards the B–N grid, and are gated into the drift region. Here they quickly establish a characteristic broad equilibrium electron energy distribution $f(\epsilon, E/N)$, where ϵ is the electron energy, and is determined by the nature of the buffer gas, the reduced electric field E/N and the ambient temperature. This distribution is considered to be spatially invariant and represents an equilibrium between the power input from the electric field and the mean rate of energy loss in collisions with the buffer gas. The $f(\epsilon, E/N)$ for various buffer gases have not been measured directly, but have been determined from solutions to the Boltzmann transport equation [33], and are accurately known for argon and nitrogen buffer gases over a wide range of E/N.

In the drift (reaction) region, an electron attaching gas (typically in concentrations of parts per million (ppm) by volume) is present. Electrons from the gated pulse, that make it to the end of the drift tube without being attached, are collected by the Faraday plate. The resulting current pulse is amplified and converted to a voltage pulse, which is then fed into a gated integrator and Boxcar averager. The signal is sampled and averaged over typically 300 pulses to yield a voltage output. Reduction of this voltage is monitored as a function of the increase in the concentration of the electron attaching gas. From this, the density normalised electron attachment coefficient, $\alpha(E/N)$, is obtained for a particular electron energy distribution, i.e. for a given E/N and temperature, using the equation:

$$V_{\text{out}} \propto \exp(-\alpha n_a L) \tag{1}$$

where n_a is the electron attaching gas number density in the drift tube of length L.

An α value for a given E/N represents the probability of electron attachment per centimetre travelled in the electric field direction per unit density of the attaching gas. The concentration of the electron attaching gas is always much less than the buffer gas concentration. Under such conditions it is assumed that $f(\epsilon, E/N)$ remains unaffected by the addition of the electron attaching gas in the drift region. The measured density normalised electron attachment coefficient is the electron attachment cross section, $\sigma(\epsilon)$, averaged over the electron energy distribution function, i.e.

$$\alpha(E/N) = \frac{1}{w(E/N)}\sqrt{\frac{2}{m_e}}\int_0^\infty \sigma(\epsilon)\sqrt{\epsilon} f\left(\epsilon, \frac{E}{N}\right) \mathrm{d}\epsilon \tag{2}$$

where m_e is the electron mass, and $w(E/N)$ is the mean electron swarm drift velocity in the buffer gas.

The electron attachment rate constant, $k_a(E/N)$ is related to $\alpha(E/N)$ by

$$k_a(E/N) = \alpha(E/N).w(E/N) \tag{3}$$

Note that α and k_a are dependent on the type of buffer gas, because the shape of the electron energy distribution is buffer gas dependent. Thus, results obtained in a nitrogen buffer gas will not necessarily be identical to those obtained in an argon buffer gas at E/N values which give the same mean electron energy. Only $\sigma(\epsilon)$ is truly

independent of buffer gas type, this being just a property of the electron attaching molecule.

To determine the anion products from electron attachment to an electron attaching molecule, a constant stream of electrons is allowed to enter the drift chamber by leaving the B–N grid continuously open. Anions, produced from the electron attachment process, drift under the influence of the electric field with considerably smaller drift velocities than electrons, towards the Faraday plate. Upon arrival at the Faraday plate, a small fraction of the anions passes through a 70 μm pinhole. These anions are then focused into a quadrupole mass spectrometer via a skimmer cone. Care is taken during this focusing to minimise collision-induced dissociation (CID) of the anions as they collide with nitrogen or argon during their acceleration into the detection region. This is achieved by keeping the voltage difference between the Faraday plate and the skimmer cone of the quadrupole mass spectrometer to a minimum, whilst maintaining good transmission of the anions. However, for certain investigations, CID can be used to some advantage; for example, to determine bond dissociation energies in the anion products [29].

In this present study we have taken the values of the electron drift velocity, w, and the mean electron energy, $\langle\epsilon\rangle$, for a given E/N in argon and nitrogen buffer gases from the data given in the papers of Hunter et al. [25,34]. Thus, the reliability and accuracy of our data critically rely on an accurate knowledge of the electron energy distribution for the buffer gas used for a given E/N in our system. As mentioned earlier our major concern is with the purity of the buffer gases we use. Standard swarm experiments use static gas conditions. Considerable care can then be taken with purifying the buffer gases. For example to purify argon, Hunter et al. [25] passed the gas first through a titanium getter heated to >600°C, stored it at liquid nitrogen temperatures and then subjected the argon to repeated freeze–pump–thaw cycles. To purify nitrogen, Hunter et al. [25,34] stored the gas at liquid nitrogen temperatures, and the vapour was extracted at just above the boiling point. Such careful procedures are not possible for an apparatus under flow conditions. Consequently, we used high purity nitrogen and argon (BOC) gases (subject to cost) in our studies, and these have stated purities of better than 99.998% and 99.9995%, respectively. The nitrogen was further purified by passing it through a liquid nitrogen trap before entering the IMS. Measurements we made of the density normalised electron attachment rate coefficients for SF_6 in a nitrogen buffer gas confirmed our assumption that minor impurities in the nitrogen buffer gas did not significantly alter the electron energy distribution $f(\epsilon, E/N)$ [29]. However, impurities in argon are more likely to cause an observable effect, where impurity levels of the order of 1 ppm have been known to significantly affect measurements [25,34]. This prompted us to measure the density normalised electron attachment coefficients for SF_6 in an argon buffer gas and compare them directly with those obtained by Hunter et al. [25]. Details of this experiment will be published later. However, for the purposes of confidence in the work presented here, we simply report that the results obtained for an argon buffer gas are, to within experimental error, in good agreement with those of Hunter et al. Thus, the impurities in our argon buffer gas, particularly N_2, CO_2, H_2O, O_2 and H_2 (all less than 1 ppm), appear to have little effect on the electron energy distribution in an argon buffer gas. In conclusion, we are confident in taking w and $\langle\epsilon\rangle$ for given E/N values from the data tables presented in the papers by Hunter et al. [25,34].

Commercial $CHCl_2F$, $CHClF_2$, and CHF_3 (Fluorochem Limited, Derbyshire, UK) were used directly without additional purification. The preparation cylinders used to store the samples of $CHCl_2F$ and $CHClF_2$, in quantities of about a few hundred ppm in a nitrogen or argon gas (depending on the buffer gas being used), were maintained at a temperature of 360 K. This was found to be necessary in order

to reduce molecular adsorption onto the walls of the cylinder which would affect the concentrations of prepared samples. Furthermore, gas chromatography measurements were made on all our samples to determine concentrations. Nevertheless, we consider that the uncertainties associated with the attaching gas number densities in the drift chamber represent the major source of error in our measurements. Taking these into account, as well as errors in electric field strengths and drift distance, we estimate the accuracy of our measurements to be ±30%.

3. Results and discussion

3.1. Density normalised electron attachment coefficients

The final voltage output (V_{out}), resulting from the electrons incident on the Faraday plate, has a simple exponential dependence on n_a (the electron attaching gas number density) as shown in Eq. (1). This simple relationship breaks down if there is an attaching gas pressure effect in the electron attachment process. Such anomalous behaviour has been observed [35], but is rare. Certainly, we did not observe any indication of high order kinetics in the electron attachment process to the two HCFCs studied in this investigation. Eq. (1) also breaks down when the assumption that the electron energy distribution is unaffected by the addition of the electron attaching gas becomes invalid, i.e. that the loss of electrons in the attachment process and energy exchange with the attaching gas molecules no longer results in a negligible perturbation on $f(\epsilon, E/N)$ [25]. In the case of SF_6, this is particularly noticeable at low E/N ($< 2 \times 10^{-19}$ V cm^2) in an argon buffer gas [25]. Nevertheless, in this study, Eq. (1) was always found to be applicable, indicating that little or no change in $f(\epsilon, E/N)$ occurred upon the introduction of either of the two HCFCs, i.e. no curvature was apparent in any plot for a given E/N in nitrogen or argon buffer gases. Thus, the $\alpha(E/N)$ values were determined from the slopes of the linear fits of the logarithm of the voltage output against n_a in the normal way [29].

For the HFC, CHF_3, the density normalised electron attachment coefficients over all mean electron energies covered in this study are smaller than the detection sensitivity of our instrument ($\alpha(E/N) \sim 10^{-18}$ cm^2).

The results of our experiments are summarised in Table 1 and Table 2 for $CHCl_2F$ and $CHClF_2$, respectively. The $\alpha(E/N)$ values for $CHCl_2F$ and $CHClF_2$ are presented in Fig. 1 as a function of mean electron energy. For comparison, the experimental data of an earlier, and to our knowledge only other, non-thermal electron energy swarm study of $CHCl_2F$ and $CHClF_2$ [9] are also presented in the figure. As one can see from the figure, there is poor agreement between the two sets of results for both $CHCl_2F$ and $CHClF_2$. This present investigation is not the only one to show inconsistencies with Lee's work. Extremely high thermal attachment rate constants have been derived from Lee's work; 1.3×10^{-9} cm^3 s^{-1} and 5.8×10^{-11} cm^3 s^{-1} for $CHCl_2F$ and $CHClF_2$, respectively [36]. These values are in disagreement to other experimental values of the thermal attachment rate constants (7.4×10^{-13} cm^3 s^{-1} [10], 1.5×10^{-12} cm^3 s^{-1} [11] for $CHCl_2F$, and $< 3.5 \times 10^{-13}$ cm^3 s^{-1} [11], $< 1.6 \times 10^{-13}$ cm^3 s^{-1} [12] for $CHClF_2$).

3.2. Electron attachment rate constants

We determined the mean electron drift velocities in argon and nitrogen buffer gases, for various E/N values, from the tables given in the papers by Hunter et al. [25,34], and used these to calculate the electron attachment rate constants for $CHCl_2F$ and $CHClF_2$.

Fig. 2 is an adapted version of a figure (Fig. 23(a)) taken from Christophorou et al.'s review [1]. The figure shows electron attachment rate constants, k_a, for a series of halogenated compounds in a nitrogen buffer gas as a function of

Table 1
Electron attachment coefficients (α) and electron attachment rate constants (k_a) for $CHCl_2F$ in N_2 and Ar buffer gases as a function of *E/N* and mean electron energy $\langle\epsilon\rangle$. The mean electron energies and mean electron drift velocities *w* for each *E/N* value in a given buffer gas have been taken from data presented in the papers of Hunter et al. [25,34]

$CHCl_2F/N_2$					$CHCl_2F/Ar$				
E/N (10^{-18} V cm^2)	$\langle\epsilon\rangle$ (eV)	$\alpha(E/N)$ (10^{-15} cm^2)	*w* (10^5 cm s^{-1})	k_a (10^{-10} cm^3 s^{-1})	*E/N* (10^{-18} V cm^2)	$\langle\epsilon\rangle$ (eV)	$\alpha(E/N)$ (10^{-15} cm^2)	*w* (10^5 cm s^{-1})	k_a (10^{-10} cm^3 s^{-1})
0.600	0.046	0.0622	1.82	0.113	0.300	0.466	2.069	1.19	2.458
1.201	0.063	0.0540	2.57	0.139	0.451	0.550	2.615	1.32	3.456
1.801	0.085	0.0685	2.81	0.193	0.601	0.624	3.012	1.43	4.296
2.395	0.108	0.0806	2.93	0.237	0.752	0.690	3.203	1.51	4.851
3.003	0.129	0.1504	3.06	0.460	1.203	0.862	3.503	1.73	6.065
3.593	0.150	0.1741	3.18	0.553	1.800	1.050	3.503	1.93	6.777
4.191	0.171	0.2380	3.32	0.791	2.399	1.208	3.022	2.08	6.287
4.790	0.190	0.3352	3.47	1.162	2.998	1.345	2.605	2.20	5.728
5.388	0.207	0.4298	3.59	1.542	3.598	1.473	1.801	2.31	4.155
5.865	0.222	0.4422	3.70	1.636	4.197	1.586	1.603	2.40	3.840
5.987	0.225	0.5155	3.72	1.919					
6.452	0.240	0.5357	3.83	2.053					
7.038	0.255	0.6605	3.94	2.601					
7.681	0.277	0.6401	4.09	2.616					
8.279	0.296	0.6941	4.20	2.918					
9.077	0.320	0.7123	4.36	3.105					
9.177	0.324	0.7305	4.38	3.199					
9.476	0.333	0.7211	4.44	3.198					
9.676	0.339	0.7220	4.47	3.229					
9.975	0.348	0.6813	4.53	3.085					

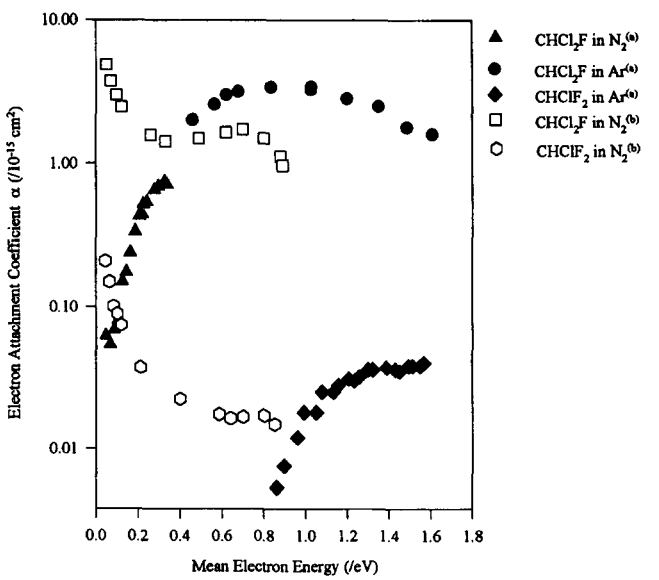

Fig. 1. The experimentally measured density normalised electron attachment coefficients (in cm^2) as a function of mean electron energy (in eV) in nitrogen and argon buffer gases for the molecules $CHCl_2F$ and $CHClF_2$, (a) our data and (b) data taken from Ref. [9]. Clearly the results from the two studies are in poor agreement.

Table 2
Electron attachment coefficients (α) and electron attachment rate constants (k_a) for $CHClF_2$ in Ar buffer gas as a function of E/N and mean electron energy $\langle\epsilon\rangle$. The mean electron energies and mean electron drift velocities w for each E/N value in the Ar buffer gas have been taken from data presented in the papers of Hunter et al. [25,34]

$CHClF_2$/Ar				
E/N (10^{-18} V cm^2)	$\langle\epsilon\rangle$ (eV)	$\alpha(E/N)$ (10^{-16} cm^2)	w (10^5 cm s^{-1})	k_a (10^{-12} cm^3 s^{-1})
1.204	0.862	0.054	1.73	0.935
1.305	0.895	0.076	1.77	1.348
1.506	0.960	0.120	1.85	2.221
1.606	0.991	0.180	1.88	3.389
1.807	1.050	0.180	1.93	3.482
1.907	1.079	0.250	1.96	4.901
2.108	1.131	0.250	2.01	5.030
2.208	1.158	0.280	2.04	5.702
2.409	1.208	0.310	2.08	6.449
2.509	1.232	0.300	2.10	6.306
2.610	1.255	0.323	2.12	6.852
2.810	1.300	0.360	2.16	7.776
2.911	1.323	0.360	2.18	7.846
3.112	1.368	0.304	2.22	6.743
3.212	1.389	0.370	2.24	8.273
3.413	1.431	0.362	2.27	8.223
3.513	1.452	0.354	2.29	8.104
3.714	1.494	0.381	2.32	8.857
3.814	1.513	0.384	2.34	8.985
4.015	1.549	0.382	2.37	9.045
4.115	1.568	0.404	2.38	9.622

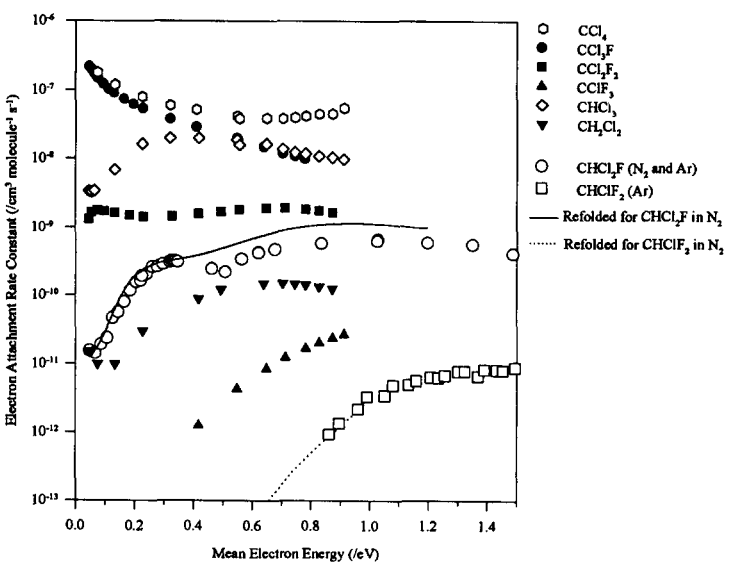

Fig. 2. An adapted version of a figure in the review by Christophorou et al. [1] showing electron attachment rate constants as a function of mean electron energy for the molecules CCl_4, CCl_3F, CCl_2F_2, $CClF_3$, $CHCl_3$, CH_2Cl_2, $CHCl_2F$ and $CHClF_2$. The solid and dotted lines give the calculated electron attachment rate constants for $CHCl_2F$ and $CHClF_2$, respectively, for a nitrogen buffer gas using the total electron capture cross sections determined in this study (see text for further details).

mean electron energy. Included on this figure are the k_a values for $CHCl_2F$ and $CHClF_2$ from this study. From the figure, and ignoring the results on the two HCFCs of this study for the present, it can be seen (as commented by Christophorou et al. [1]) that the effect of increasing the number of Cl atoms in the halogenated methane results in a marked increase in the electron attachment rate constant, as also does replacement of H by F for a given number of chlorine atoms. (Only for mean electron energies above 0.6 eV does this rule break down between two of the molecules, with the electron attachment rates of $CHCl_3$ becoming slightly greater than those for CCl_3F.) If the rule applies to $CHCl_2F$, its electron attachment rate constants should be greater than those for CH_2Cl_2 but less than those for CCl_2F_2, and indeed this is found to be the case, as can be seen from Fig. 2. The rule is also obeyed for $CHClF_2$, for which the electron attachment rate constants are less than those for $CClF_3$ over all the mean electron energies studied.

Extrapolation of our electron attachment rate constant data to $\langle\epsilon\rangle = 0$ approximates a value of 6.7×10^{-12} cm^3 s^{-1} for the thermal electron attachment rate constant, k_{th} for $CHCl_2F$. A more detailed calculation using Eq. (2), but with $f(\epsilon, E/N)$ replaced by a 300 K Maxwellian energy distribution and using the electron capture cross sections determined from our rate data (see below), gives $k_{th} = 6.2 \times 10^{-12}$ cm^3 s^{-1}. These values are comparable, although slightly higher, than the two previously reported values [10,11].

The results presented by Christophorou et al. [1] have all been taken in one buffer gas, nitrogen, up to a mean electron energy of 1 eV [1]. Our results, on the other hand, have been taken in nitrogen only up to a mean electron energy of 0.4 eV. To go to higher mean electron energies, we had to operate our system in an atmospheric pressure of argon gas. Although, in many studies the k_a values as a function of mean electron energy taken in nitrogen and argon buffer gas do smoothly mesh with one another [1] (for example, SF_6 [25]), in the case of $CHCl_2F$ this is not true, and this is illustrated in Fig. 2. Thus, care must be taken when comparing electron attachment rate constants measured in a nitrogen buffer gas with those measured in an argon buffer gas. This results from differences in $f(\epsilon, E/N)$ (even if one operates the swarm experiment so that the mean electron energy is the same in the two cases). Nevertheless, k_a values can be calculated for any buffer gas provided that the electron capture cross section $\sigma(\epsilon)$ and $f(\epsilon, E/N)$ are known. An unfolding procedure was adopted to determine $\sigma(\epsilon)$, and this is now briefly described.

3.3. A determination of the electron attachment cross sections $\sigma(\epsilon)$

A knowledge of the electron attachment rate constant $k_a(E/N)$ and how it varies as a function of E/N is important for many applications. However, generally such information is of limited physical value because of its strong dependence on buffer gas type. The electron capture cross section, $\sigma(\epsilon)$, on the other hand, is a more physically significant quantity, being independent of buffer gas type.

Eq. (2) provides a means to determine $\sigma(\epsilon)$ through a swarm unfolding technique, which was originally developed by Christophorou and coworkers [23,37]. For this determination, the electron energy distribution $f(\epsilon, E/N)$ needs to be known at each E/N for which $k_a(E/N)$ values have been determined. In this work, we assumed that the electron energy distribution is given by a Druyvesteyn distribution [38]:

$$f(\epsilon, E/N) = C\epsilon^{1/2}\exp\left[\frac{-B\delta\epsilon^2}{\lambda_e^2 e^2 E^2}\right] \quad (4)$$

where C is a normalising constant, $\delta = 2m_e/m$ (m_e being the electron mass, and m being the mass of a buffer atom (argon) or molecule (nitrogen)), λ_e is the electron mean free path, and e is the electron charge. Clearly the electron energy distributions can be changed by varying the applied electric field strength E along the drift tube. λ_e is dependent on the momentum transfer cross

sections. These cross sections for the purpose of our calculations, were taken from those reported by Hunter and Christophorou [34] for nitrogen and Milloy et al. [39] for argon. The B in the exponential was adjusted to give mean electron energies equal to those given in the papers by Hunter et al. [25,34] for either pure nitrogen or argon buffer gases at various E/N values. The resulting $f(\epsilon, E/N)$ values were then used in Eq. (2) and an iterative procedure, similar to that established by Christophorou et al. [37], was adopted which allowed $\sigma(\epsilon)$ to be unfolded from the measured $k_a(E/N)$ values.

For this study the iteration for the swarm unfolding continued until a best-fit between the calculated electron attachment rate constants and those determined from a smooth curve fitted to the experimental values was obtained. It should be noted that, generally, we find the number of iterations has little affect on the position of the peak(s) in the electron capture cross section, but does affect the widths and height of the peak(s).

Tests in the reproducibility of the iterative procedure adopted were performed by refolding computer simulated cross sections to give $\alpha(E/N)$ values, and then swarm unfolding these to determine the cross sections. We found that the widths and intensities of the peaks of the cross sections from the unfolded data reproduced the computer simulated peaks extremely well, with a high degree of accuracy. Generally, the iteration is carried out until the difference in the term

$$R_n = \Sigma_j[\alpha_{exp}(E/N)_j - \alpha_{calc}(E/N)_j]^2 / \Sigma_j[\alpha_{exp}(E/N)_j]^2 \quad (5)$$

is a minimum, n being the number of iterations [23]. However, we found it necessary to continue the iterative procedure until the quantity $(R_{n+1} - R_n)/R_n) \approx 10^{-5}$. This removed the difficulty when no clear minimum occurred, and an asymptotic limit was being reached. The validity of this approach was further verified by taking sets of electron attachment rate constants for various halogenated molecules reported in the literature, using our unfolding procedure to obtain electron attachment cross sections, and then comparing these with those already published. Generally the agreement between our $\sigma(\epsilon)$ and those already reported is good. By way of an example of the quality and reliability of the unfolding procedure, Fig. 3 illustrates the electron attachment cross sections for two CFCs, CCl_2F_2 and CCl_3F that we obtained using the electron attachment rate constants from the work of McCorkle et al. [23]. On the same figure are electron attachment cross sections calculated by McCorkle et al. [23]. Clearly, there is fair agreement between the two calculations, with the same general features observed in both. Slight discrepancies in the peak positions, heights and widths can be attributed to differences in the electron energy distributions and the number of iterations used.

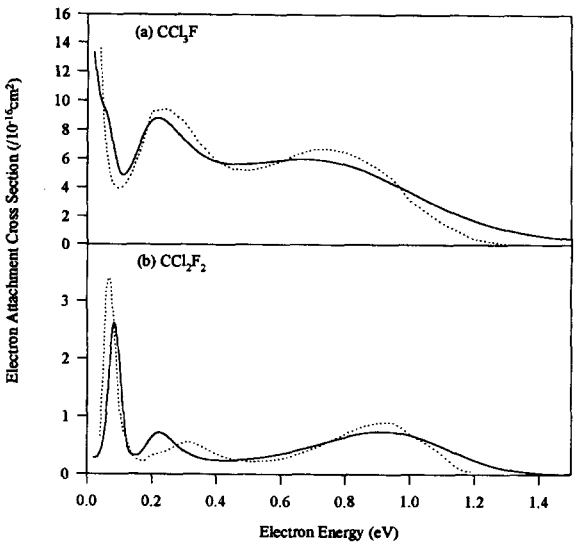

Fig. 3. Our swarm unfolding procedure applied to the electron attachment rate constants of (a) CCl_3F and (b) CCl_2F_2 taken from the work of McCorkle et al. [23]. The momentum transfer cross sections for N_2 [34] and Ar [39] were used to determine the electron energy distribution at every E/N. The solid lines represent our calculated $\sigma(\epsilon)$ and the dotted line those of McCorkle et al. [23]. Fair agreement exists between the two unfolding procedures. Slight discrepancies can be associated with differences in the electron energy distribution adopted.

The results of the swarm unfolding technique applied to our measured $k_a(E/N)$ values for

$CHCl_2F$ and $CHClF_2$ are presented in Fig. 4(a) and 4(b), respectively. Two broad peaks appear in the $\sigma(\epsilon)$ curve for $CHCl_2F$; a small one has its maximum at approximately 0.4 eV and the other (more dominant) one at approximately 1.2 eV. The cross section values taken for this study were the ones for which the fractional difference in the errors in consecutive iterations were not significantly changed, i.e. $(R_{n+1} - R_n)/R_n \approx 10^{-5}$. To illustrate the quality of the fitting procedure, the $\sigma(\epsilon)$ values have been used in a folding procedure to determine the electron attachment rate constants as a function of E/N. This is shown in Fig. 5(a). The lower curve represents the electron attachment rate constants measured in a nitrogen buffer gas and the upper one in an argon buffer gas. In partial agreement with our calculations, by using an electron beam method, Hickam and Berry [40] found a maximum in the Cl^- current at an electron energy of 0.8 eV. This is close to, but lower in energy than the value

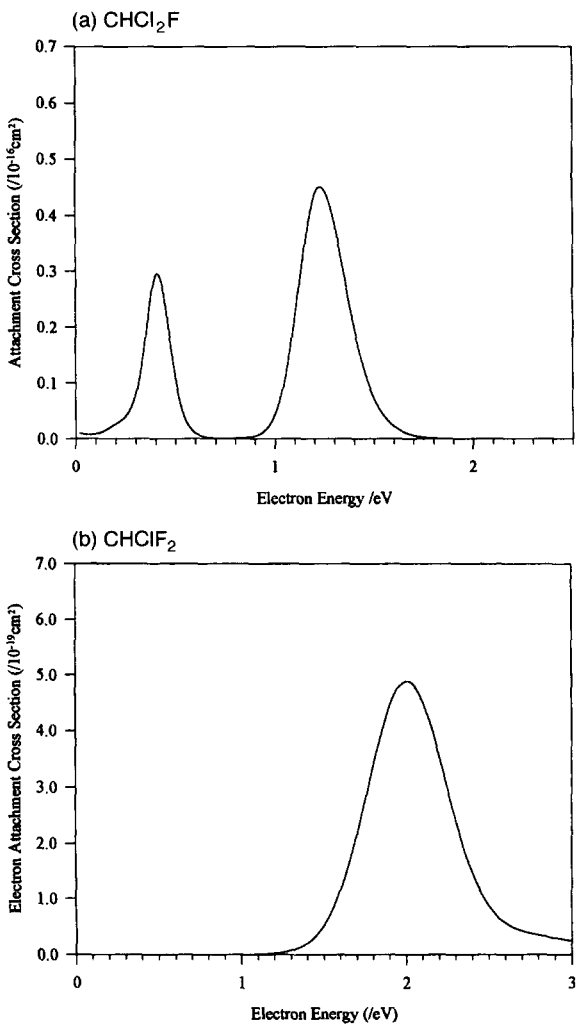

Fig. 4. The total electron attachment cross section, $\sigma(\epsilon)$, as a function of electron energy determined for (a) $CHCl_2F$ and (b) $CHClF_2$ obtained using an unfolding procedure using our measurements of the electron attachment rate constants as described in the text.

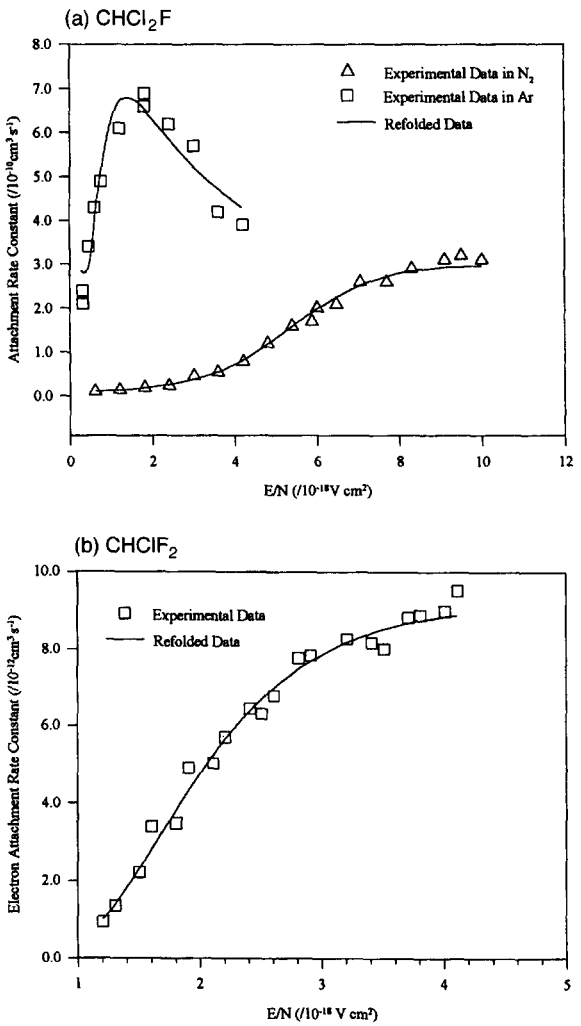

Fig. 5. The electron attachment rate constants as a function of E/N, determined using the calculated $\sigma(\epsilon)$ values in a folding procedure as discussed in the text and represented by solid lines for (a) $CHCl_2F$ and (b) $CHClF_2$, compared to the measured values in argon (□) and nitrogen (△).

obtained by us for the dominant peak in our $\sigma(\epsilon)$ curve. However, Hickam and Berry used the formation of SF_6^- to establish the electron energy scale, and this is known to generally underestimate the energy [21].

The $\sigma(\epsilon)$ determined for $CHCl_2F$ have been used in a folding procedure to calculate the k_a values in a nitrogen buffer gas over a greater mean electron energy (up to about 1.2 eV) than is possible in our direct measurements. These are represented by the solid line in Fig. 2. It can be seen that the calculated electron attachment rate constants for $CHCl_2F$ in a nitrogen buffer gas are greater than those measured in an argon buffer gas at the same mean electron energy. This serves to illustrate the point made earlier, that care must be taken when comparing electron attachment rate constants at the same mean electron energy taken in different buffer gases.

Unfolding of the $CHClF_2$ electron attachment rate constants resulted in just one peak in the $\sigma(\epsilon)$ curve at approximately 2 eV, and this is shown in Fig. 4(b). The calculated $\sigma(\epsilon)$ for $CHClF_2$ have been used in a folding procedure to obtain $k_a(\langle\epsilon\rangle)$ in a nitrogen buffer gas, and these results are represented by the dotted line in Fig. 2, which in this case smoothly mesh in with the argon data. Furthermore, the folding procedure has been used to obtain $k_a(E/N)$ in an argon buffer gas to compare with the experimental values, and this is illustrated in Fig. 5(b).

3.4. Mass spectra

In general, low energy electron attachment to CFCs and chlorinated methanes is dissociative, i.e. a short-lived excited parent anion is formed, which dissociates to yield a fragment anion together with a neutral (usually a radical) fragment. This is illustrated in Table 3, which summarises the results from a number of studies of electron attachment [41–46]. Most of these results were obtained using crossed beam techniques to CCl_4, CCl_3F, CCl_2F_2, $CClF_3$, $CHCl_3$ and CH_2Cl_2. Clearly, Cl^- is the most abundant anion produced following electron attachment. Other anions are observed, but at much smaller intensities and for much higher electron energy than for Cl^-. The two HCFC molecules presented in this study are expected to display dissociative electron attachment. This is confirmed from mass spectra of the anion products resulting from the electron attachment process, and subsequent anion–molecule reactions, under swarm conditions. Fig. 6 illustrates a typical mass spectrum obtained for $CHCl_2F$. A number of m/z values are apparent in the spectrum. Cl^- (m/z = 35 and 37 found in the natural isotope abundance ratio of 3:1) is the primary anion resulting from electron attachment to $CHCl_2F$. That no parent anion is observed implies that either a bound ground state of $CHCl_2F^-$ does not exist, or if it does, the lifetime of the excited $CHCl_2F^-$ anion is too short for collisional stabilisation to occur (see below) and that redistribution of the excess energy from electron attachment to the various vibrational modes of $CHCl_2F^-$ does not occur. Thus, the total electron attachment rate constants and cross sections are for the dissociative pathway:

$$e^- + CHCl_2F \rightarrow Cl^- + CHClF$$

In agreement with this, the electron beam study of $CHCl_2F$ showed Cl^- to be the only anion product [40]. That Cl^- is the dominant anion found from electron attachment to chlorine-containing halocarbons is expected because the electron affinity of the Cl atom generally exceeds the C–Cl bond dissociation energy.

When high concentrations of $CHCl_2F$ are injected, the Cl^- (which is the primary product of electron attachment) associates with $CHCl_2F$, to form $CHCl_2F.Cl^-$, i.e. it is a secondary product resulting from an anion–molecule reaction. Other minor peaks are also due to anion reactions with impurities in our system, e.g. $Cl^- + H_2O \rightarrow Cl^-.(H_2O)$. Only a peak observed in the mass spectrum (see Fig. 6) at m/z = 96 remains unassigned.

For $CHClF_2$, Cl^- is the only primary anion, and no association product with $CHClF_2$ is observed.

Table 3
Summary of results from various studies (Refs. [41–46]) of the anion products of electron attachment to several chlorine containing methanes. Electron attachment to these molecules always leads to dissociative products. Note that the peak intensities are normalised to the Cl^- peak for each molecule

Molecule	Negative ion	Relative peak or energy integrated intensity	Peak energy (eV)
CCl_4	Cl^-	1000 [a, b, c]	<10 meV [b] 0 [c] 0.75 [c]
	Cl_2^-	8 [c]	1.1 [c]
	CCl_2^-	0.5 [c]	1.65 [c] 6.0 [c]
	CCl_3^-	4 [c]	1.3 [c]
$CClF_3$ [d, e]	F^-	200 (500)	4.1 (4.3)
	Cl^-	1000 (1000)	1.3 4.8(1.4) (5.0)
	FCl^-	200 (10)	3.9 (4.7)
	CF_2Cl^-	80 (75)	4.2 (4.4)
CCl_2F_2 [d]	F^-	138	3.1
	Cl^-	1000	0.55
	FCl^-	22	2.85
	Cl_2^-	21	0.65
	$CFCl_2^-$	43	3.55
CCl_3F [d]	F^-	5	3.0
	Cl^-	1000	0.0
	Cl_2^-	1.2	1.6
	CCl_3^-	0.4	3.3
$CHCl_3$ [c, f]	Cl^-	1000 (1000)	0.32(0.35)
	Cl_2^-	(0.1)	(~1.8)
	HCl_2^-	2.5	1.6
	CCl_2^-	0.8	1.45
	$CHCl_2^-$	(1)	(~1.7)
CH_2Cl_2 [c]	Cl^-	1000	0.05
	Cl_2^-	12	1.25
	CCl_2^-	2	1.4

a–f are Refs. [41–46], respectively. Ref. [41] uses collisions with high Rydberg state K(np) atoms, and Ref. [42] involves a technique of threshold photoionisation of krypton atoms. The rest are from electron beam studies.

Thus to summarise, for both molecules the electron attachment process is as follows:

$$e^- + CHCl_xF_{3-x} \rightarrow (CHCl_xF_{3-x}^-)^* \rightarrow Cl^- + CHCl_{x-1}F_{3-x}$$

where $x = 1$ or 2. For thermal electrons, the enthalpy of this reaction process is -51 ± 10 kJ mol^{-1} for $CHCl_2F$ and $+20 \pm 10$ kJ mol^{-1} for $CHClF_2$. In the case of $CHCl_2F$, Cl^- can associate with the parent molecule:

$$Cl^- + CHCl_2F \rightarrow Cl^-.CHCl_2F$$

Obviously, the relative intensities of the Cl^- and $Cl^-.CHCl_2F$ peaks in the mass spectrum are dependent on the $CHCl_2F$ concentration. The mass spectrum given in Fig. 6 was taken with a concentration of $CHCl_2F$ (0.4 ppm) which shows both the primary anion product from the electron attachment process and the product of the subsequent anion–molecule association reaction. With sufficient $CHCl_2F$ number density in the drift chamber, the Cl^- peak in the mass spectrum disappears and only one dominant peak corresponding to $Cl^-.CHCl_2F$ remains.

A small signal at m/z ~82 is observed in the electron attachment mass spectrum of $CHCl_2F$ (see Fig. 6). This could be CCl_2^-. If this assignment is correct, a high resolution mass spectrum should show three peaks, with m/z values and relative abundances of 82(9), 84(6) and 86(1). Unfortunately, the ion current was not sufficient to permit a high resolution mass spectrum to be obtained. There are no exothermic anion–molecule reactions of Cl^- with $CHCl_2F$ which

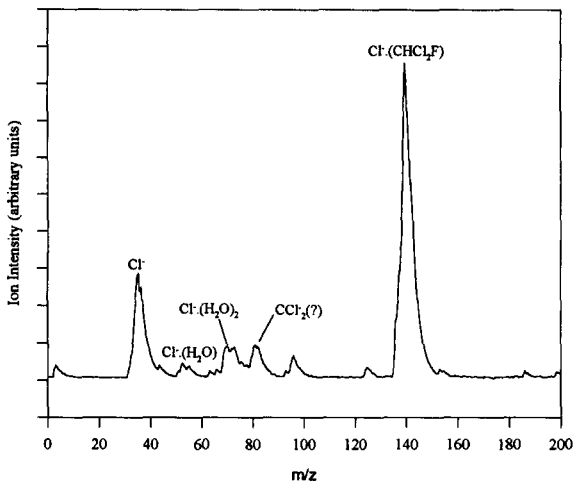

Fig. 6. A typical mass spectrum resulting from electron attachment to $CHCl_2F$. Similar spectra were obtained for all *E/N* values in both nitrogen and argon buffer gases. For the spectrum presented, a nitrogen buffer gas was used with $E/N = 5.88 \times 10^{-18}$ V cm^2 and a $CHCl_2F$ concentration of 0.4 ppm. The dominant peak resulting from electron attachment is that of the anion Cl^-. Cl^- can then associate with the parent neutral molecule to form $Cl^-.CHCl_2F$. The minor peaks in the mass spectrum are, we propose, due to anion reactions with trace impurities present in our system, although the peak at $m/z \sim 82$ could be CCl_2^-.

lead to CCl_2^-. For example, the reaction pathway

$$Cl^- + CHCl_2F \rightarrow CCl_2^- + HF + Cl$$

is endothermic by 414 kJ mol^{-1}. (The thermochemical data used to determine the enthalpy of the reaction was taken from the compilation by Lias et al. [47] for the heats of formation of Cl^-, $CHCl_2F$, HF and Cl, and from Refs. [48,49] for electron affinity and heat of formation of CCl_2, respectively.) To confirm that Cl^- does not have a bimolecular reaction with $CHCl_2F$, a separate study was undertaken using a selected ion flow tube (SIFT). The SIFT apparatus, experimental technique, and analysis of data have been extensively reviewed [50] and the reader is referred to that reference for more details. Fig. 7(a) shows a mass spectrum of the Cl^- anions injected into the SIFT. $^{35}Cl^-$ was preferentially injected. A mass spectrum of the products from the $Cl^-/CHCl_2F$ reaction is given in Fig. 7(b). This clearly shows three peaks corresponding to the three major isotopomers of $CHCl_2F.Cl^-$ at m/z = 137, 139

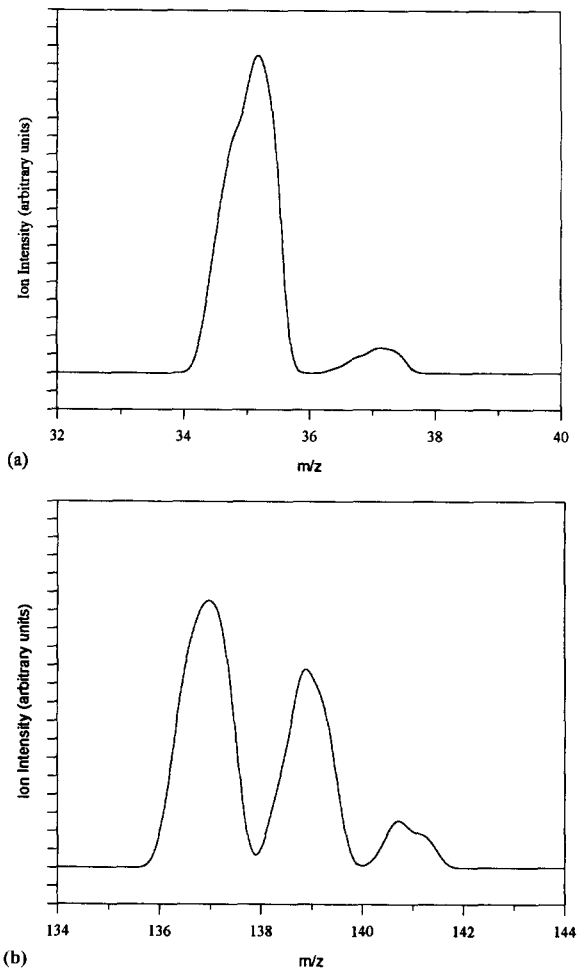

Fig. 7. Results from a selected ion flow tube (SIFT) investigation of the reaction of Cl^- with $CHCl_2F$. Mass spectra of (a) the Cl^- anions injected into the flow tube and (b) the anion product $Cl^-.CHCl_2F$ resulting from the association reaction of Cl^- with $CHCl_2F$. No other anion products from the reaction were observed. Note that the resolution of the injection quadrupole for this experiment was sufficiently low to allow both $^{35}Cl^-$ and $^{37}Cl^-$ anions to enter the flow tube. However, $^{35}Cl^-$ was preferentially injected, as is indicated by the heights of the peaks given in (a).

and 141. These data show that Cl^- reacts exclusively by association with $CHCl_2F$, with the stabilisation of the product in the SIFT presumably being achieved by collisions with helium atoms. No other anion products were observed.

The above results therefore suggest that, if it is formed, CCl_2^- can only be from dissociative

electron attachment:

$$e^- + CHCl_2F \rightarrow CCl_2^- + HF$$

$$\Delta H = 66 \pm 12 \text{ kJ mol}^{-1}$$

For which the enthalpy has been calculated for thermal electrons. The endothermicity corresponds to 0.68 eV. Thus, attachment of electrons with energies above this value can yield the CCl_2^- product. This corresponds to the dominant resonance in the cross section curve.

The m/z = 82 signal is very weak, and may have come from an impurity in the sample. In the electron beam study of $CHCl_2F$ [40] only Cl^- was detected. It should be noted that CCl_2^- is formed by dissociative electron attachment to some chlorinated methanes (see Table 3), but the yield of CCl_2^- is always considerably less than that of the Cl^-. It is possible that CCl_2^- could have been overlooked in the electron beam study.

Finally, our identification of Cl^- (and possibly CCl_2^-) as the product of electron attachment to $CHCl_2F$ has implications for the results presented in the paper of Szamrej et al. [10]. In their paper, it is suggested that, through an 'unknown process', CO_2 assists electron attachment to $CHCl_2F$, and that this three-body mechanism is far more efficient than simple two-body dissociative attachment. Their apparatus had no facilities for anion identification. At present, our experiments are performed under flowing buffer gas conditions at constant atmospheric pressure, so we are unable to perform any measurements to check for buffer gas pressure effects. We do know the product, and no rearrangement of the transient anion (in this case $(CHCl_2F^-)^*$) is necessary to form Cl^- [51]. Dissociation of $(CHCl_2F^-)^*$ will be fast compared to collisional stabilisation, even in an atmospheric pressure buffer gas. The rate of dissociative electron attachment to form Cl^- should be independent of the total pressure [1,39,52]. Based on our identification of Cl^- as the product, we can offer no explanation for the strong increase of the electron attachment rate constant of $CHCl_2F$ with increasing CO_2 buffer gas pressure reported by Szamrej et al. [10]. Further investigations of the identification of the product anions formed when CO_2 is used as the buffer gas may help to explain their results.

4. Concluding remarks

For the three molecules studied here, it is observed that as the number of Cl atoms decreases (from 2 to 0), the electron attachment rate constant dramatically decreases, with CHF_3 having no measurable electron attachment rate constants, within the sensitivity of our instrument, over the mean electron energy range 0.05–1.8 eV. These results agree with the general trend suggested by Christophorou et al. [1], and the electron attachment rate constants have values consistent with those of other related halogenated compounds, i.e. over the mean electron energy range covered in Fig. 23(a) of Christophorou et al.'s review [1], 0 to ~1 eV:

$$k_a(CCl_2F_2) > k_a(CHCl_2F) > k_a(CH_2Cl_2)$$

and $k_a(CClF_3) > k_a(CHClF_2) > k_a(CHF_3)$

The electron attachment rate constants obtained in this study exhibit large discrepancies from those obtained by Lee [9]. Lee's electron attachment rate constants increase with decreasing mean electron energy, whereas ours show the opposite trend. Furthermore, the thermal electron attachment rate constant we estimated for $CHCl_2F$, 6.2×10^{-12} cm^3 s^{-1}, is significantly less than that obtained from the swarm study of Lee [36], but comparable to the value obtained by Szamrej et al. [10], 7.4×10^{-13} cm^3 s^{-1}, and the value obtained by Christodoulides et al. [11], 1.5×10^{-12} cm^3 s^{-1}. Independent measurements, for instance using the FALP technique, would be of interest.

From our measured electron attachment rate constants of $CHCl_2F$ and $CHClF_2$, the electron capture cross sections as a function of electron energy have been derived by an unfolding

technique. From these calculations there are two resonances for electron attachment to $CHCl_2F$ and one resonance for $CHClF_2$ between 0 and 4 eV. For both molecules the dominant anion product resulting from the electron attachment process is Cl^-. To our knowledge, only an electron beam study of $CHCl_2F$ has been performed [40], showing a maximum in the Cl^- current at an electron energy of 0.8 eV. Problems with energy calibration and resolution in the beam study make an accurate comparison between the beam studies and ours impossible. Thus, other measurements of $\sigma(\epsilon)$ are needed to confirm the electron attachment cross sections we have generated from our electron attachment rate constants. We hope that this work will stimulate such studies.

Mass spectra have shown that electron attachment to $CHCl_2F$ and $CHClF_2$ is a two-body dissociative process, predominantly yielding Cl^-. This is in agreement with the electron beam study of $CHCl_2F$ [40]. Cl^- is not a unique anion which can be used to identify these two molecules. Thus, direct electron attachment cannot be used to monitor these compounds in the environment. However, the secondary process of the association reaction of the primary product anion, Cl^-, with $CHCl_2F$, resulting in $Cl^-.CHCl_2F$, does produce a unique fingerprint to the detection of $CHCl_2F$. This would provide a suitable and sensitive method of monitoring this molecule.

Finally, this study is of general interest, because dissociative electron attachment to chlorine containing molecules is of importance for many applications, such as plasma etching [52], gaseous dielectrics [53], optically controlled diffuse discharge switches [54] and ionospheric chemistry [55].

Acknowledgements

We are extremely grateful to PLSD (CBD), Porton Down, for the grant which provided funds to build the apparatus, and for the continuing support of Drs P. Watts and K. Giles at the PLSD (CBD). We thank Dr. Richard Kennedy for a number of useful discussions and Dr. R. Peverall for the initial development of the program used for the determination of cross sections from electron attachment rate constants. GKJ thanks NERC for providing a research studentship. SMS is indebted to the Office of International Relationships of N.H.R.F. through which he received a Royal Society grant to visit the Chemical Physics Laboratory of Birmingham University. LS was funded through an EC network program (CEC Contract CHRX-CT94-0485). We thank Mr. George Roupakas (N.H.R.F., Theoretical and Physical Chemistry Institute, Athens, Greece) for his assistance in taking some of the measurements. We should like to thank the Head of the School of Physics and Space Research, Professor G. C. Morrison, for providing funds for Mr. Roupakas's visit. Finally we are indebted to Mr. G. Burns (School of Chemistry, University of Birmingham) for his assistance with the GC measurements.

References

[1] L.G. Christophorou D.L. McCorkle, A.A. Christodoulides, in L.G. Christophorou (ed.), Electron–Molecule Interactions and their Applications, Academic Press, Orlando, 1984, Vol. I, Chapter 6.
[2] Z.L. Petrovic, W.C. Wang, L.C. Lee, J. Chem. Phys. 90 (1989) 3145.
[3] H.X. Wan, H.H. Moore, J.A. Tossell, J. Chem. Phys. 94 (1991) 1868.
[4] P. Rowntree, L. Sanche, L. Parenteau, M. Meinke, F. Weik, E. Illenberger, J. Chem. Phys. 101 (1994) 4248.
[5] T.U. Lemons, T.J. Gergei, J.H. Moore, J. Chem. Phys. 102 (1995) 119.
[6] R.A. Popple, C.D. Finch, K.A. Smith, F.B. Dunning, J. Chem. Phys. 104 (1996) 8485.
[7] WMO, 1990 World Meteorological Organization Global Ozone Research and Monitoring Project Report No 20, Volume I, Geneva, Switzerland.
[8] R.F. Warren, A.R. Ravishankara, Int. J. Chem. Kinetics 25 (1993) 179.
[9] T.G. Lee, J. Phys. Chem. 67 (1963) 360.
[10] I. Szamrej, W. Tchorzewska, H. Kosc, M. Forys, Radiat. Phys. Chem. 47 (1996) 269.

[11] A.A. Christodoulides, R. Schumacher, R.W. Schindler, Int. J. Chem. Kinetics 10 (1978) 1215.
[12] F.J. Davis, R.N. Compton, D.R. Nelson, J. Chem. Phys. 59 (1973) 2324.
[13] D. Smith, N.G. Adams, E. Alge, J. Phys. B: Atom. Mol. Phys. 17 (1984) 461.
[14] E. Alge, N.G. Adams, D. Smith, J. Phys. B: Atom. Mol. Phys. 17 (1984) 3827.
[15] D. Smith, C.R. Herd, N.G. Adams, Int. J. Mass. Spec. Ion Processes 93 (1989) 15.
[16] D. Smith, C.R. Herd, N.G. Adams, J.F. Paulson, Int. J. Mass. Spec. Ion Processes 96 (1990) 341.
[17] T.M. Miller, A.E.S. Miller, J.F. Paulson, X. Liu, J. Chem. Phys. 100 (1994) 8841.
[18] C.L. Chen, P.J. Chantry, J. Chem. Phys. 71 (1979) 3897.
[19] M. Fenzlaff, R. Gerhard, E. Illenberger, J. Chem. Phys. 88 (1988) 149.
[20] S.M. Spyrou, I. Sauers, L.G. Christophorou, J. Chem. Phys. 78 (1983) 7200.
[21] L.G. Christophorou, Atomic and Molecular Radiation Physics, Wiley-Interscience, New York, 1971.
[22] L.G. Christophorou, D.L. McCorkle, J.G. Carter, J. Chem. Phys. 54 (1971) 253.
[23] D.L. McCorkle, A.A. Christodoulides, L.G. Christophorou, I. Szamrej, J. Chem. Phys. 72 (1980) 4049.
[24] S.M. Spyrou, L.G. Christophorou, J. Chem. Phys. 83 (1985) 641.
[25] S.R. Hunter, J.G. Carter, L.G. Christophorou, J. Chem. Phys. 90 (1989) 4879.
[26] P.G. Datskos, L.G. Christophorou, J.G. Carter, J. Chem. Phys. 99 (1993) 8607.
[27] E.C.M. Chen, J.R. Wiley, C.F. Batten, W.E. Wentworth, J. Phys. Chem. 98 (1994) 88.
[28] A. Chutjian, A. Garscadden, J.M. Wadehra, Physics Reports 264 (1996) 393.
[29] Y. Liu Y, C.A. Mayhew, R. Peverall, Int. J. Mass. Spec. Ion Processes 152 (1996) 225.
[30] H.H. Hill Jr., W.F. Siems, R.H. Louis, D.G. McMinn, Anal. Chem., 62 (1990) 1201A (and references cited therein).
[31] P. Watts, Int. J. Mass. Spec. Ion Processes 121 (1992) 141.
[32] C.J. Hayhurst, P. Watts, A. Wilders, Int. J. Mass. Spec. Ion Processes 121 (1992) 127.
[33] L.G.H. Huxley, R.W. Crompton, The Diffusion and Drift of Electrons in Gases, Wiley-Interscience, New York, 1974.
[34] S.R. Hunter, L.G. Christophorou, J. Chem. Phys. 80 (1984) 6150.
[35] S.R. Hunter, L.G. Christophorou, D.L. McCorkle, I. Sauers, H.W. Ellis, D.R. James, J. Phys D: Appl. Phys. 16 (1983) 573.
[36] R.P. Blaustein, L.G. Christophorou, J. Chem. Phys. 49 (1968) 1526.
[37] L.G. Christophorou, D.L. McCorkle, V.E. Anderson, J. Phys. B: Atom. Mol. Phys. 4 (1971) 1163.
[38] E.W. McDaniel, Collision Phenomena in Ionized Gases, Wiley, New York, 1964.
[39] H.B. Milloy, R.W. Crompton, J.A. Rees, A.G. Robertson, Aust. J. Phys., 30 (1977) 61.
[40] W.M. Hickam, D. Berry, J. Chem. Phys. 29 (1958) 517.
[41] R.A. Popple, C.D. Finch, K.A. Smith, F.B. Dunning, J. Chem. Phys. 104 (1996) 8485.
[42] A. Chutjian, S.H. Alajajian, Phys. Rev. A 31 (1985) 2885.
[43] H.U. Scheunemann, E. Illenberger, H. Baumgartel, Ber. Bunsenges. Phys. Chem. 84 (1980) 580.
[44] E. Illenberger, H.U. Scheunemann, H. Baumgartel, Chem. Phys. 37 (1979) 21.
[45] S.M. Spyrou, L.G. Christophorou, J. Chem. Phys. 82 (1985) 2620.
[46] J.P. Johnson, L.G. Christophorou, J.G. Carter, J. Chem. Phys. 67 (1977) 2196.
[47] S.G. Lias, J.E. Bartmess, J.F. Liebman, J.L. Holmes, R.D. Levin, W.G. Mallard, J. Phys. Chem. Ref. Data, (Suppl. 1) (1988) 17.
[48] K.K. Murray, D.G. Leopold, T.M. Miller, W.C. Lineberger, J. Chem. Phys. 89 (1988) 5442.
[49] D.W. Kohn, E.S.J. Robles, C.F. Logan, P. Chen, J. Phys. Chem. 97 (1993) 4936.
[50] D. Smith, N.G. Adams, Adv. Atom. Mol. Phys. 24 (1988) 1.
[51] D.L. McCorkle, L.G. Christophorou, S.R. Hunter, in L.G. Christophorou (ed.), Electron and Ion Swarms, Pergamon Press, 1982, pp. 21–33.
[52] A.D. Richards, B.E. Thompson, K.D. Allen, H.H. Sawin, J. Appl. Phys. 62 (1987) 792.
[53] R.J. VanBrunt, J. Appl. Phys. 61 (1987) 1773.
[54] L.G. Christophorou, S.R. Hunter, J.G. Carter, R.A. Mathis, Appl. Phys. Lett. 41 (1982) 147.
[55] B.J. Finlayson-Pitts, J.N. Pitts, Jr., Atmospheric Chemistry, Wiley-Interscience, New York, 1986.